Biochimica et Biophysica Acta 939 (1988) 197–206
Elsevier

BBA 73946

Current transients generated by the Na^+/K^+-ATPase after an ATP concentration jump: dependence on sodium and ATP concentration

R. Borlinghaus and H.-J. Apell

Department of Biology, University of Constance, Constance (F.R.G.)

(Received 8 October 1987)

Key words: ATPase, Na^+/K^+-; ATP concentration jump; Current transient; caged ATP

Planar membrane fragments containing a high density of oriented Na^+/K^+-ATPase molecules are bound to planar lipid bilayers. ATP is released in the aqueous solution within milliseconds from an inactive, photolabile precursor ('caged ATP') by an intense light flash. By this ATP-concentration jump a large number of pump molecules is activated almost simultaneously. Charge translocation in the pump molecule results in a voltage transient which is recorded in the external measuring circuit. From the voltage signal, the intrinsic pump current $I_p(t)$ can be evaluated using information on the circuit parameters of the compound membrane system. The pump current $I_p(t)$ is compared with the results of numerical simulations of a reaction cycle derived from the Post-Albers reaction scheme combined with the photochemical release reaction of caged ATP. The time course of I_p can be satisfactorily fitted using kinetic parameters of the Na^+/K^+-ATPase from the literature. The dependence of I_p on sodium concentration c_{Na} can be described using a single set of kinetic parameters in which only c_{Na} is varied. I_p as a function of c_{Na} is well fitted by a first-order Michaelis-Menten type equation with $K_m \approx 4$ mM. This finding is consistent with the assumption that two sodium binding sites have a high affinity and that a third site of lower affinity is rate limiting. The ATP concentration dependence of I_p is studied by varying the concentration of caged ATP in the solution and the yield of photochemical release of ATP.

Introduction

The Na^+/K^+-ATPase in the plasma membrane of animal cells promotes active transport of sodium and potassium ions coupled to ATP hydrolysis [1–7]. Under physiological conditions more Na^+ is moved outward than K^+ inward, meaning that the Na^+/K^+-pump operates in an electrogenic mode. The net movement of charge during the pump cycle generates a current whose analysis yields mechanistic information of the Na^+/K^+-ATPase [8–11]. For the investigation of pump currents mainly steady-state experiments have been carried out so far [12–17]. The use of 'caged' ATP which allows to perform ATP concentration jumps opened up the possibility to study nonstationary states of the pump from which additional kinetic information may be obtained [18–21,34].

In earlier publications [21,22] we described experiments, in which mechanistic properties of the transport cycle were studied by measuring the current response after an ATP concentration jump. In this paper we investigate the sodium and ATP concentration dependence of the current response and show that a complete description of observed transport phenomena is possible on the basis of the Post-Albers reaction model of the pump.

Correspondence: H.-J. Apell, Fakultät für Biologie, Universität Konstanz, D-7750 Konstanz, F.R.G.

Materials and Methods

Materials. L-1,2-Diphytanoyl-3-phosphatidylcholine was obtained from Avanti Polar Lipids Inc., Birmingham, AL; sodium dodecylsulfate (SDS) from Pierce Chemical Company, Rockford, IL, and sodium cholate from Merck, Darmstadt. Phospho*enol*pyruvate, pyruvate kinase, lactate dehydrogenase, luciferin, luciferase, NADH and ATP (disodium salt, Sonderqualität) were from Boehringer, Mannheim. Apyrase VI, ouabain and dithiothreitol were purchased from Sigma. NaCl was used in suprapure quality (Merck). All other reagents were analytical grade. P^3-1-(2-nitro)phenylethyladenosine 5′-triphosphate ('caged' ATP) was synthetized by K. Janko using a modified version of the method of Kaplan et al. [26]. The purity of the product was checked by HPLC. The compound was stored as a tetramethylammonium salt in the dark at −40 °C.

Preparation of Na^+/K^+-ATPase. Flat membrane sheets containing Na^+/K^+-ATPase in high density were prepared according to the method of Jørgensen [23]. The enzyme activity (ATP hydrolysis) determined by a combined assay [24] was about 2000 μmol inorganic phosphate per h and mg protein at 37 °C. The sheet preparations could be stored at −70 °C in 100-μl samples for up to 2 years without significant loss of activity. Storage of the thawed preparation at +4 °C did not affect the activity within 5 weeks.

Membrane experiments. Planar lipid bilayers were formed from 1% diphytanoyl phosphatidylcholine in *n*-decane [25]. The cell (Fig. 1) which was machined from black teflon, was mounted in a Faraday cage in a thermostated metal block. The potential across the bilayer was detected using Ag/AgCl-electrodes in both electrolyte compartments and a voltage amplifier with 10^{12} Ω input impedance and a gain of 20. The electrodes were shielded with carbon blackened agar-agar against stray-light artefacts. Na^+/K^+-ATPase and caged ATP were added to this 'cis' compartment. The 'trans' compartment was sealed and was equipped with a poly(vinylchloride) screw for volume adjustment. Ultraviolet light from a flash bulb with known intensity profile passed a glass filter (Schott UG11, 1 mm) and was focussed on the membrane through a quartz window (Fig. 1). The cis-compartment which had a volume of approx. 300 μl was equipped with a small magnetic stirrer. The buffer solution contained, if not indicated otherwise, 150 mM NaCl, 20 mM $MgCl_2$, 20 mM dithiothreitol and 50 mM Tris-HCl (pH 7.0), 20 mM Mg^{2+} were chosen to obtain reproducible current amplitudes. Below 5 mM Mg^{2+} the current amplitudes varied strongly between different experiments. A possible explanation may be that the adsorption of membrane fragments is promoted by higher Mg^{2+} concentrations. The form of the signal or the kinetic parameters do not vary in the investigated concentration range between 1 mM and 100 mM. After equilibration the experiments were started with injection of variable amounts of caged ATP and 40 μg/ml protein to the cis-side, followed by 45 s of smooth stirring. Voltage-traces were recorded after 40 μs ultraviolet flashes. The waiting times between flashes were chosen to be 10 min in order to guarantee complete hydrolysis of liberated ATP [21].

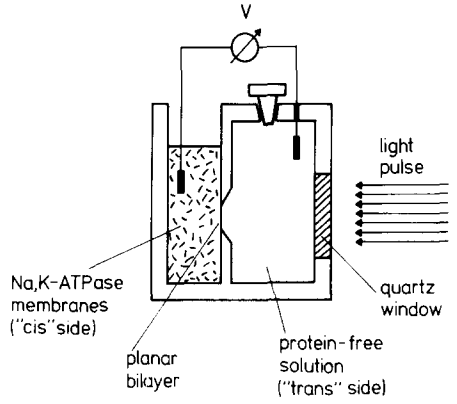

Fig. 1. Membrane cuvette for measuring voltage signals from optically black lipid membranes with adsorbed Na^+/K^+-ATPase membrane fragments. The 'trans' compartment was closed after filling with the solution. The solution volumes of the open and the closed compartment were 0.3 and 5 ml, respectively; the diameter of the circular membrane was approx. 1.3 mm. A magnetic stirrer (not shown) was present in the 'cis'-compartment. The solutions were connected to the external measuring circuit via agar bridges and silver/silver-chloride electrodes. In order to minimize stray-light artefacts from the electrodes, a suspension of carbon black was added to the agar.

Determination of liberated ATP. At pH 7.0 ATP is liberated from caged ATP with a time constant of 4.6 ms [27]. In the absence of dithiothreitol the

signal amplitudes slowly declined after repeated flashes, presumably as a result of reactions of photoproducts with the protein [21].

The concentration of flash-released ATP near the membrane surface was estimated in the following way. In the presence of a lipid membrane in the cuvette but in the absence of protein a series of flashes in intervals of 5 seconds was applied to a solution of 1.5 mM caged ATP under continuous stirring. After every 10 flashes a small sample of the solution (1 μl) was removed and analyzed with a luciferase assay in a LKB-luminometer [28]. Due to the high molar absorption coefficient ($\varepsilon = 26\,900\ M^{-1} \cdot cm^{-1}$) at 260 nm the light intensity is strongly attenuated along the optical pathlength in the cuvette. Calibration experiments were performed to determine the degree of light absorption behind the membrane in the 'cis'-compartment at the given spectral intensity of the flash lamp and the given filter characteristics. The action spectrum of caged ATP was determined separately. The light-flash passed through a normalized monochromator (Jobin-Yvon, H 10 VIS) and was focussed on a quartz-cuvette, containing 0.5 mM caged ATP. After 50 flashes under continuous stirring the ATP-concentration was determined with the luciferase-assay. Folding the absorption and action spectrum numerically and using the Lambert-Beer law, the concentration profile of liberated ATP along the light path in the cuvette was calculated in wavelength intervals of 5 nm.

The concentration of ATP in the aliquots taken from the cuvette represents an average over the original concentration profile with the cross-section of the membrane hole in the (black) teflon cuvette. By integration of the Lambert-Beer law, the yield, θ, of liberated ATP was estimated to be about 13% at full light intensity within the first 20 μm behind the membrane. With an estimated diffusion coefficient of ATP of $3 \cdot 10^{-6}\ cm^2 \cdot s^{-1}$ this means that the ATP concentration in front of the membrane would remain constant for 1.5 s.

Results

Voltage signals after an ATP-concentration jump

After the UV-flash, the voltage starts to increase, reaching a maximum at approx. 200 ms, and thereafter decreases to a quasi-stationary value

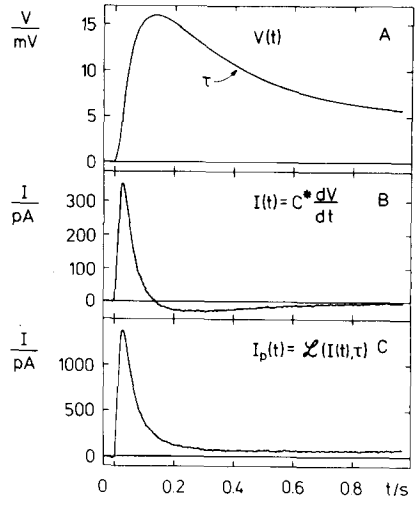

Fig. 2. (A) Transmembrane voltage $V(t)$ after a light flash at time $t = 0$. The aqueous solutions contained 150 mM NaCl, 50 mM Tris-HCl (pH 7.0) 20 mM dithiothreitol and 20 mM $MgCl_2$. $T = 20\,°C$. 0.5 mM caged ATP and 12 μg Na^+/K^+-ATPase fragments were added to the 'cis' compartment 20 min prior to the flash experiment. The positive sign of the voltage corresponds to a translocation of positive charge from the membrane fragments towards the black lipid membrane. The decay of the voltage after the maximum shows a single exponential behaviour with the time constant τ. (B) Time derivative $dV(t)/dt$ of the voltage signal obtained numerically from the voltage signal given in part A of the figure. According to Ref. 20, dV/dt is proportional to the short circuit current $I(t)$. The capacity C^* is approximately equal to the capacity of the black lipid bilayer [21]. (C) Intrinsic pump current $I_p(t)$ calculated from $I(t)$ by transformation with the operator $\mathscr{L}(I(t), \tau)$ according to the method described in Ref. 21.

(Fig. 2a). In the preceding paper [21] it was shown that the derivative of the voltage signal $U(t)$ is proportional to the current transient across the bilayer sheet system; the proportionality factor being given by the capacitance of the black film (Fig. 2b). As shown previously, the current signal $I(t)$ determined by numerical derivation of the voltage signal $U(t)$ can be transformed into the pump current $I_p(t)$ by numerical treatment taking the circuit properties of the compound membrane system into account (Fig. 2c). The transformation operator $\mathscr{L}(I(t), \tau)$ is derived in Ref. 21:

$$\mathscr{L}(I(t), \tau) = 4.3 \cdot \left\{ I(t) + (1/\tau) \int_0^t I(t)\, dt \right\}$$

I_p shows a maximum at a time t_1 and decreases

with a time constant τ_I to a stationary value I_p^∞ (Fig. 2).

As shown previously [22], transient currents can be calculated by a numerical simulation of a pump cycle for the Na^+-ATPase derived from the Post-Albers reaction model using rate constants and equilibrium constants which are in good agreement with published data obtained by various methods and from different tissues. The analysis performed in Apell et al. [22] reduced the complex time-course of ATP release from caged ATP to a single time constant. This simplified treatment was valid under the condition of a fixed concentration of caged ATP and a fixed light intensity. Since in the present analysis both parameters have been varied in order to get different concentrations of liberated ATP, it is necessary to combine the pump cycle (in the absence of potassium) and the release kinetics of ATP after photoactivation (see Appendix A). The corresponding reaction scheme is shown in Fig. 3. The lower part represents the pump cycle in the absence of potassium and the upper part the reaction kinetics of caged ATP. X stands for caged ATP and Y for the activated state of caged ATP. Activation of caged ATP can occur in the enzyme-bound state of the molecule ($E_1X \rightarrow E_1Y$), as well as in solution ($X \rightarrow Y$). Both reactions may be assumed to be fast (up to 5 μs) compared to other reaction steps [27]. Binding and unbinding of caged ATP to the enzyme is described by rate constants z_f, z_b, y_f and y_b (Fig. 3). We assume the association-dissociation process not to be affected by photoexcitation of caged ATP ($z_f = y_f$, $z_b = y_b$). λ and λ_E are the rate constants of the monomolecular decay of caged ATP to ATP in the free and in the enzyme-bound state, respectively. We assume λ_E and λ to be approximately equal, with $\lambda = 220\ s^{-1}$ at pH 7.0. The kinetic parameters of the further reactions, binding and occlusion of Na, phosphorylation of the enzyme, $E_1 \rightarrow E_2$ transition and release of Na and inorganic phosphate have been used as described by Apell et al. [22].

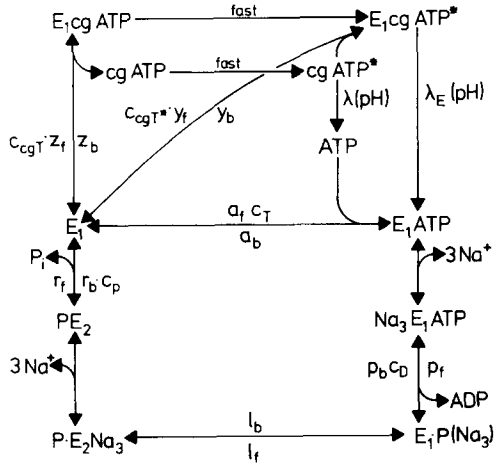

Fig. 3. Reaction scheme of the system containing caged ATP and Na^+/K^+-ATPase in the absence of potassium, based on the Post-Albers model of the pumping cycle. E_1 and E_2 are conformations of the enzyme with ion binding sites exposed to the cytoplasmic and to the extracellular side, respectively. In the 'occluded' state $(Na_3)E_1$-P, the bound ions are unable to exchange with the aqueous solutions. cgATP refers to caged ATP, and cgATP* to its photochemical intermediate. c_T, c_{cgT}, c_{cgT*}, c_D and c_p are the cytoplasmic concentrations of ATP, caged ATP, the photochemical intermediate, ADP and inorganic phosphate. $a_f c_T$, $z_f c_{cgT}$, $y_f c_{cgT*}$, p_f, l_f, r_f and a_b, z_b, y_b, $p_b c_D$, l_b, $r_b c_p$ are rate constants for transitions in forward and backward direction, respectively. P_i, inorganic phosphate.

A typical experiment (500 μM caged ATP, 150 mM NaCl) is shown in Fig. 4. It is found that the calculated curve can be well fitted to the experimental $I_p(t)$ by slight variation of the parameters a_f, l_f. The rate constants z_f and z_b have been held fixed in all experiments at $3 \cdot 10^6\ s^{-1} \cdot M^{-1}$ and $1500\ s^{-1}$, resulting in appropriate fits of the rise of the transient current. These constants lead to $K_d = z_b/z_f = 5 \cdot 10^{-4}$ M, a value which is about 10-times larger than the value of K_d given in Ref. 18. The time to reach the current maximum, t_1, and the time constant, τ_I, of the almost exponential decay turned out to be well-defined empirical parameters, which may be used to characterize an experiment and to compare the observed time course of I_p with the result of the numerical simulation. t_1 and τ_I are complicated functions of all rate constants which cannot be given analytically. In opposite to the signal amplitude I_{peak} the time constants t_1 and τ_I are not functions of the number of active pump molecules in the experiment.

Dependence on sodium concentration

To vary the sodium concentration, buffers with

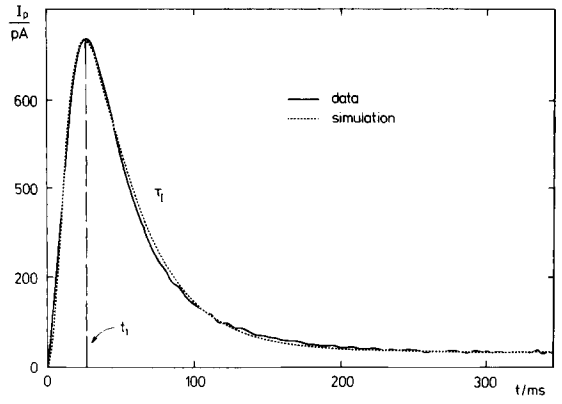

Fig. 4. Pump current $I_p(t)$ compared with numerical simulations based on the reaction scheme of Fig. 3. Experimental conditions are the same as in Fig. 2. The simulation was carried out with $c_{cgT} = 0.5$ mM, $\theta = 0.13$, $c_D = c_P = 0$, $[Na^+] = 150$ mM, $K_{Na} = 4$ mM, $z_f = y_f = 3 \cdot 10^6$ $M^{-1} \cdot s^{-1}$, $z_b = y_b = 1500$ s^{-1}, $\lambda = \lambda_e = 220$ s^{-1}, $a_f = 2.3 \cdot 10^6$ $M^{-1} \cdot s^{-1}$, $a_b = 23$ s^{-1}, $p_f = 200$ s^{-1}, $l_f = 27$ s^{-1}, $l_b = 2.1$ s^{-1}, $r_f = 0.27$ s^{-1}.

different contents of Na were used. After one or two experiments with this 'starting' buffer, the sodium concentration was increased by adding a small volume of a 3 M NaCl solution. Increasing the Tris-concentration from 50 mM to 250 mM at [Na] = 5 mM did not influence the signal, indicating that effects of ionic strength are negligible. In

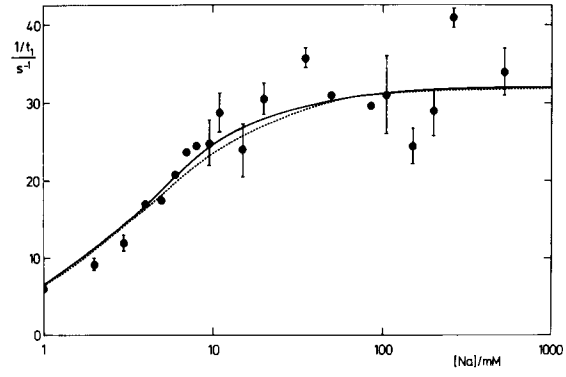

Fig. 5. Sodium-concentration dependence of the empirical parameter $1/t_1$. The data points are the average of at least three experiments. Error bars indicate the scatter of data. $T = 20$ °C. The solid line is the result of a simulation with the parameters given in the legend of Fig. 4. Only the sodium concentration $[Na^+]$ is varied. The dashed line corresponds to a first-order Michaelis-Menten kinetics with $K_m = 4$ mM.

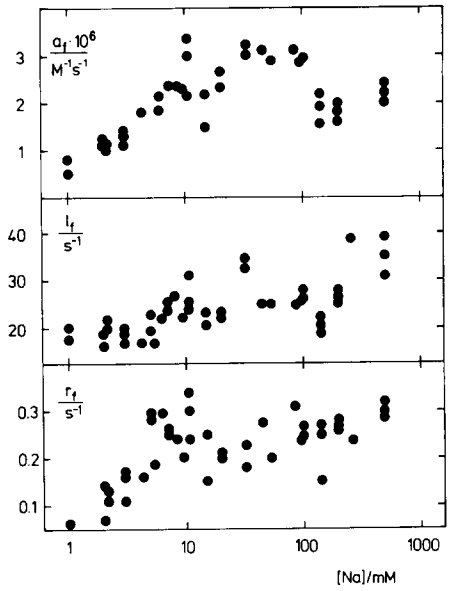

Fig. 6. Values of the kinetic parameters a_f, l_f and r_f at different sodium concetrations for which an optimum fit is obtained. The corresponding equilibrium constants a_f/a_b, l_f/l_b and r_f/r_b have been kept constant. The same data as given in Fig. 5 have been used.

most experiments the Tris concentration was kept at 50 mM.

Fig. 5 shows the effect of the sodium concentration on the empirical parameter $1/t_1$ (filled circles). For the numerical simulation of the reaction scheme (Fig. 3) all kinetic parameters except the sodium concentration were kept constant. The τ_l values show the same agreement between experiment and simulation. τ_l varied between 670 ± 50 ms ($[Na^+] = 1$ mM) and 35 ± 5 ms ($[Na^+] = 500$ mM). When, in addition, the rate constants belonging to the partial reactions of the pump cycle were varied in order to obtain optimum fits, only slight variations were necessary in the forward rate constants a_f, l_f and r_f, at constant values of the ratios a_f/a_b, l_f/l_b and r_f/r_b (Fig. 6).

Influence of liberated ATP

The amount of liberated ATP is determined by two parameters: the total concentration of initially present caged ATP, and the fraction θ of caged ATP which is transformed into ATP in a single flash. θ is a function of light intensity. The maximum value of θ which was achieved with our experimental set-up was 13% at the location of the

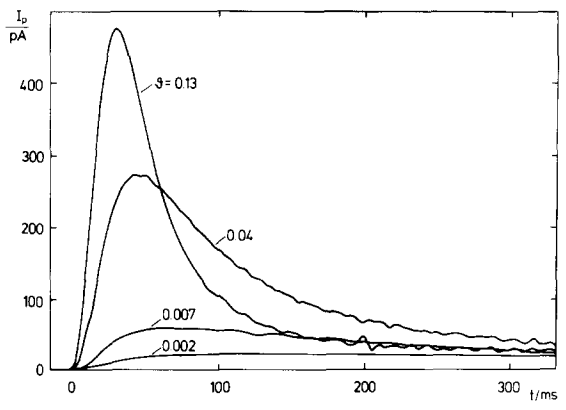

Fig. 7. Variation of pump current $I_p(t)$ with incident light intensity. The yield θ of liberated ATP at the membrane surface in the 'cis' compartment is controlled by varying the light intensity between 100% ($\theta = 0.13$), 31% ($\theta = 0.04$), 5.4% ($\theta = 0.007$), 1.5% ($\theta = 0.002$). The concentration of caged ATP is 1.5 mM.

membrane. Using wire nets of different mesh size, the light intensity could be reduced to 1.5%. Fig. 7 shows experiments at a caged ATP concentration of 1.5 mM for different values of θ. It is seen from

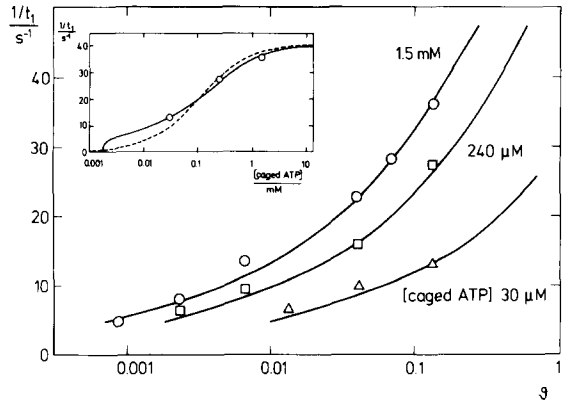

Fig. 8. Influence of the concentrations of caged ATP and liberated ATP on the empirical parameter $1/t_1$. At three different concentrations of caged ATP (○, 1.5 mM; □, 240 µM; △, 30 µM) the light intensity was varied to generate yields of liberated ATP between 0.001 and 0.13. $T = 20\,°C$. The lines were obtained by numerical simulation with the parameters given in legend of Fig. 4. Only c_{cgT} and θ are varied. The inset shows the dependence of $1/t_1$ on the concentration of caged ATP at a θ of 0.13. The solid line is calculated using the parameter values given in the legend of Fig. 4. The dashed line represents a fit of the Michaelis-Menten equation ($K_m = 0.1$ mM).

Fig. 7 that below a certain concentration of liberated ATP the maximum in $I_p(t)$ disappeared. In Fig. 8 experimental values of $1/t_1$ are compared with the results of simulations for three different concentrations of caged ATP. In the calculated curves only the concentration of caged ATP and θ are varied according to experimental conditions; all other parameters are kept constant. The τ_I values show the same agreement between experiment and simulation.

Discussion

The comparison of experimental results and numerical simulations confirm, as suggested in the previous paper [22], that a pump cycle derived from the Post-Albers reaction scheme is able to describe the electrical signals generated by the electrogenic pumping activity of the Na^+/K^+-ATPase in the absence of K^+. The kinetic parameters used in the reaction scheme (Fig. 3) do not differ significantly from published data [11]. Although the set of parameters used is not unique, variation of parameters is clearly restricted, as can be seen from Fig. 6. A significant change in one parameter cannot be compensated by variation of the other parameters, since the influence of a given parameter is different during the time-course of the signal.

The well-studied photochemistry of caged ATP [27] allows a correct description of the observed ATP and the caged ATP concentration dependence by coupling the enzyme kinetics with the kinetics of the ATP release as shown in Fig. 3.

Sodium concentration dependence

The variation of sodium ion concentration over almost three orders of magnitude led to a significant change in the shape of the voltage signal. The time to reach the peak current decreases from 170 ms ($[Na^+] = 1$ mM) to 30 ms ($[Na^+] = 500$ mM). Numerical simulations according to the pump cycle were found to describe the behaviour of both empirical parameters t_1 and τ_I satisfactorily. In Fig. 5 the experimental data and the results from the simulation are compared with the predictions from Michaelis-Menten type kinetics. The implementation of the sodium binding into the mathematical formalism [11,22] is based on the

assumption that sodium ions bind independently to the three cytoplasmic sites so that the equilibrium dissociation constants K_{Na1}, K_{Na2}, K_{Na3} are related to the dissociation constant K_{Na} by:

$$K_{Na1} = \tfrac{1}{3}K_{Na}; \quad K_{Na2} = K_{Na}; \quad K_{Na3} = 3K_{Na}$$

K_{Na} was chosen to be 4 mM [11,22]. As shown in Fig. 5, the comparison between simulation and first-order Michaelis-Menten kinetics reveals a strong similarity in shape when $K_m = K_{Na} = 4$ mM. Second- and third-order kinetics do not fit the experimental results.

In Fig. 3 an ordered binding of ATP and Na^+ is assumed although random binding of both substrates is reported in the literature [35]. Since the electrogenic step(s) do not occur before the sodium occluded state $E_1P(Na_3)$ [21,22], and ATP and caged ATP have similar binding constants [18], and since the binding of ATP is not influenced significantly by the Na^+ concentration [36], the restriction on an ordered binding does not change the time-course of the simulated current signal.

These findings may be compared with other studies of the effects of Na^+ concentration reported in the literature. Fendler et al. [19] estimated by a similar method the binding constant K_m to be 7 mM in the Na-only-mode of the Na^+/K^+-ATPase. Garay and Garrahan [29] and Blostein [30] used red cells and found S-shaped concentration dependences for Na–Na-exchange in the absence of potassium, indicating cooperativity of the binding sites. The corresponding binding constants K_{Na} were 3.2 mM [29] and 0.31 mM [30]. Forgac and Chin [31] and Karlish et al. [32] investigated Na^+/K^+-ATPase from kidney reconstituted in lipid vesicles. In the absence of potassium both groups found hyperbolic dependence of the transport rate on Na^+ concentration with K_m values of 1 mM [31] and 2 mM [32]. These results closely agree with our findings. A possible explanation for the observed first-order kinetics is the assumption that two of the three binding sites are negatively charged and the third site is neutral [32,33]. For electrostatic reasons the affinity of sodium at the neutral side should be reduced so that binding to this site becomes rate limiting. This would lead to first-order Michaelis-Menten kinetics. The difference between red cells and reconstituted kidney enzyme may result from differences in protein structure.

ATP concentration dependence

Caged ATP binds to the Na^+/K^+-ATPase without being hydrolyzed. The fact that ATP and caged ATP compete for the same binding site [18], complicates the study of ATP-concentration effects on charge translocation. Three different processes contribute to the current transient which mainly consists of the one turnover of the pump: (1) caged ATP bound to the enzyme is converted in situ and reacts immediately; (2) ATP which is converted in solution binds to unoccupied enzyme; and (3) ATP competes with caged ATP bound to the enzyme. Only the latter mechanism can be described by stationary inhibition kinetics. The rate constants for binding and dissociation of caged ATP, which were determined from simulations fitting our experiments, give an equilibrium dissociation rate constant in the range of $5 \cdot 10^{-4}$ M. At a caged ATP concentration of 1.5 mM 75% of the ATP binding sites should be occupied by caged ATP under the conditions of our experiments prior to the flash. The maximum yield θ of liberated ATP was 13%. Therefore, the same concentration of ATP caused different pumping currents when produced by different yields θ and starting concentrations of caged ATP. 30 μM caged ATP and $\theta = 0.13$ produced 3.9 μM ATP, which in turn leads to a value of $t_1 = 75$ ms. The same ATP concentration produced by 1.5 mM caged ATP and $\theta = 0.003$ generated a value of $t_1 = 122$ ms. Since the above-mentioned nonstationary components contribute significantly to the current transient the data as well as the simulations cannot be described by equilibrium kinetics as shown in the inset of Fig. 8.

The fit by numerical calculation (Fig. 8) shows that the reaction scheme of Fig. 3 which includes competition between ATP and caged ATP satisfactorily describes the experimental observations. Therefore it is possible to compare the binding constants used for the fit with values published in the literature. The binding constants for caged ATP and ATP are 500 μM and 10 μM, respectively, which leads to a ratio of both constants of 50. Forbush published affinities for the binding of caged ATP and ATP in the absence of Mg^{2+} of 43

μM and 0.5 μM respectively, which gives a ratio of 86 [18]. Nagel and co-workers [34] performed experiments with a technique similar to ours and analysed the results assuming competition between ATP and caged ATP under equilibrium conditions. Neglecting the contribution of the conversion of caged ATP bound to the enzyme (up to 30% of first turnover) they determined a binding constant for caged ATP to be 30 μM [34] and a ratio of the binding constants of 15, which allowed to calculate a binding constant for ATP in the range of 2 μM [34]. The most striking difference can be seen in the binding constant for caged ATP. It should be emphasized that the values of our binding constants are tentative, since they have not been determined directly, as it was done by Forbush [18], but they have been obtained by fitting a system of interdependent kinetic parameters. The information of these experiments, nevertheless, is that interaction of ATP, caged ATP and enzyme can be described in the whole range of experiments by the kinetic scheme shown in Fig. 3, which is part of the Post-Albers cycle.

Appendix A

Analysis of nonstationary pump-currents: numerical simulation based on the reaction cycle of Fig. 3

After sudden release of ATP a sequence of transitions is initiated between discrete states P_1, $P_2, \ldots,$ P_M of the pump molecule with rate constants k_f^i and k_b^i of the ith elementary reaction step in forward and backward direction of the transition $P_i \rightarrow P_{i+1}$. When x_i is the fraction of pump molecules in the state P_i, the net rate Φ_i of this transition is given by

$$\Phi_i = x_i k_f^i - x_{i+1} k_b^{i+1} \tag{A-1}$$

The contribution of this net rate Φ_i to the charge translocation in the external measuring circuit depends on the dielectric coefficient α_i, a microscopic parameter which describes the charge movement belonging to transition $P_i \rightarrow P_{i+1}$:

$$\alpha_i = \gamma_i a_i / d \tag{A-2}$$

where $\gamma_i e_0$ (e_0 is the elementary charge) is the equivalent charge that moves over a distance a_i in a homogenous dielectric layer of thickness d. The α_i fulfil the boundary condition

$$\sum_i \alpha_i = \nu \tag{A-3}$$

in which ν is the number of elementary charges translocated from one aqueous phase to the other during one pump cycle [22].

The macroscopic pump current may be presented as

$$I_p(t) = e_0 N \cdot \sum_i \alpha_i \Phi_i(t) \tag{A-4}$$

N is the number of pump molecules in the membrane. A more detailed discussion of the meaning of the α_i can be found in Apell et al. [22]. Analysis of the reaction scheme of Fig. 3 leads to the following description. For calculation of time dependent net rates $\Phi_a(t)$, $\Phi_p(t), \ldots,$ $\Phi_r(t)$ we denote the fraction of pump molecules in state A by $x[A]$ and introduce the following variables

$$x_1 = x[E_1] \tag{A-5}$$

$$x_2 = x[E_1 \cdot ATP] + x[NaE_1 \cdot ATP] + x[Na_2E_1 \cdot ATP] + x[Na_3E_1 \cdot ATP] \tag{A-6}$$

$$x_3 = x[(Na_3)E_1P] \tag{A-7}$$

$$x_4 = x[P-E_2] + x[P-E_2Na] + x[P\text{-}E_2Na_2] + x[P-E_2Na_3] \tag{A-8}$$

$$x_5 = x[E_1X] \tag{A-9}$$

$$x_6 = x[E_1Y] \tag{A-10}$$

$$\sum_{i=1}^{6} x_i = 1 \tag{A-11}$$

According to Apell et al. [22], the time derivatives of the variables x_i are given by:

$$\dot{x}_1 = -\left[c_x^0\{(1-\theta)z_f + \theta e^{-\lambda t} y_f + \theta(1-e^{-\lambda t})a_f\} + c_p r_b + y_b\right] x_1 + (z_b - y_b)x_5 + \left(r_f \frac{1}{P''} - y_b\right)x_4 + \left(\frac{a_b}{P'} - y_b\right)x_2 + y_b x_3 + y_b \tag{A-12}$$

$$\dot{x}_2 = \left\{ a_f c_x^0 \theta (1-e^{-\lambda t}) - \lambda_E \right\} x_1 - \left(a_b \frac{1}{P'} + p_f \frac{n_1' n_2' n_3'}{P'} + \lambda_E \right) x_2 + (p_b c_D - \lambda_E) x_3 - \lambda_E (x_4 + x_5) + \lambda_E \quad \text{(A-13)}$$

$$\dot{x}_3 = p_f \frac{n_1' n_2' n_3'}{P'} x_2 + (p_b c_D - l_f) x_3 + l_b \frac{n_1'' n_2'' n_3''}{P''} \quad \text{(A-14)}$$

$$\dot{x}_4 = r_b c_p x_1 + l_f x_3 - \left(l_b \frac{n_1'' n_2'' n_3''}{P''} + r_f \frac{1}{P''} \right) x_4 \quad \text{(A-15)}$$

$$\dot{x}_5 = a_f c_x^0 (1-\theta) x_1 - z_b x_5 \quad \text{(A-16)}$$

x_6 is obtained from Eqn. A-11. θ is the fraction of caged ATP which is converted into the photochemical intermediate Y by the light flash (Fig. 1). P' and n_i' are given by

$$P' \equiv 1 + n_1' + n_1' n_2' + n_1' n_2' n_3' \quad \text{(A-17)}$$

$$n_i' = [\mathrm{Na}]'/K'_{\mathrm{Na}_i} \quad \text{(A-18)}$$

P'' and n_i'' are defined in an analogous way. $'$ stands for the cytoplasmic side and $''$ for the extracellular side. $K^j(\mathrm{Na}_i)$ are the equilibrium constants for sodium binding.

Eqns. A-12–A-16 are numerically integrated with the appropriate initial conditions.

The time dependence of the concentration of caged ATP, $c_X = c_{cgT}$, of the photochemical intermediate, c_Y, and of ATP, c_T, is given by

$$c_X = c_X(t<0) \cdot (1-\theta) = c_X^0 (1-\theta) \quad \text{(A-19)}$$

$$c_Y = \theta c_X^0 e^{-\lambda t} \quad \text{(A-20)}$$

$$c_T = \theta c_X^0 (1-e^{-\lambda t}) \quad \text{(A-21)}$$

The (normalized) initial conditions are (immediately after the flash)

$$x_1(t=0) = 1/(1+K_X c_X^0) \quad \text{(A-22)}$$

$$x_5(t=0) = (K_X c_X^0 (1-\theta))/(1+K_X c_X^0) \quad \text{(A-23)}$$

$$x_6(t=0) = (K_X c_X^0 \theta)/(1+K_X c_X^0) \quad \text{(A-24)}$$

$$x_2 = x_3 = x_4 = 0 \quad \text{(A-25)}$$

$K_X = z_f/z_b$ is the equilibrium association constant of E_1X. From the solution of this system of differential equations the pump current I_p is calculated to be

$$I_p/Ne_0 = \alpha_a \Phi_a + \alpha' (\Phi_1' + \Phi_2' + \Phi_3') + \alpha_p \Phi_p + \alpha_l \Phi_l + \alpha'' (\Phi_1'' + \Phi_2'' + \Phi_3'') + \alpha_r \Phi_r \quad \text{(A-26)}$$

The dielectric factors, α_a, α', α_p, α_l, α'' and α_r, are exactly as used in Eqn. 13 in Ref. 22.

$$\Phi_a = (a_f c_T + z_f c_X + y_f c_Y) x_1 - \left(a_b \frac{1}{P'} x_2 + z_b x_5 + y_b x_6 \right) \quad \text{(A-27)}$$

$$\Phi_p = p_f \frac{n_1' n_2' n_3'}{P'} x_2 - p_b c_D x_3 \quad \text{(A-28)}$$

$$\Phi_l = l_f x_3 - l_b \frac{n_1'' n_2'' n_3''}{P''} x_4 \quad \text{(A-29)}$$

$$\Phi_r = r_f \frac{1}{P''} x_4 - r_b c_p x_1 \quad \text{(A-30)}$$

$$\Phi_Y = \lambda_E x_6 \quad \text{(A-31)}$$

$$\Phi_1' + \Phi_2' + \Phi_3' = \frac{1}{P'} \left\{ (\Phi_a + \Phi_Y) n_1' (1 + 2n_2' + 3n_2' n_3') + \Phi_p (n_2' n_1' + 2n_1' + 3) \right\} \quad \text{(A-32)}$$

$$\Phi_1'' + \Phi_2'' + \Phi_3'' = \frac{1}{P''} \{ \Phi n_r'' (1 + 2n_2'' + 3n_2'' n_3'') + \Phi_l (n_2'' n_1'' + 2n_1'' + 3) \} \quad \text{(A-33)}$$

Acknowledgements

We thank Dr. P. Läuger for stimulating discussions and support. This work has been financially supported by the Deutsche Forschungsgemeinschaft (Sonderforschungsbereich 156).

References

1 Skou, J.C. (1975) Q. Rev. Biophys. 7, 401–431.
2 Robinson, J.D. and Flashner, M.S. (1979) Biochim. Biophys. Acta 549, 145–176.
3 Cantley, L.C. (1981) Curr. Top. Bioenerg. 11, 201–237.
3 Schuurmans-Stekhoven, F. and Bonting, S.L. (1981) Physiol. Rev. 61, 1–76.
5 Jørgensen, P.L. (1982) Biochim. Biophys. Acta 694, 27–68.
6 Glynn, I.M. (1985) in The Enzymes of Biological Membranes, 2nd Edn., vol. 3: Membrane Transport (Martonosi, ed.), pp. 35–114, Plenum Press, New York.
7 Kaplan, J.H. (1985) Annu. Rev. Physiol. 47, 535–544.
8 Hansen, U.-P., Gradmann, D., Sanders, D. and Slayman, C.L. (1981) J. Membrane Biol. 63, 165–190.

9 De Weer, P. (1984) in Electrogenic Transport: Fundamental Principles and Physiological Implications (Blaustein, M.P. and Lieberman, M., eds.), pp. 1–15, Raven Press, New York.
10 Reynolds, J.A., Johnson, E.A. and Tanford, Ch. (1985) Proc. Natl. Acad. Sci. USA 82, 6869–6873.
11 Läuger, P. and Apell, H.-J. (1986) Eur. Biophys. J. 13, 309–321.
12 Abercrombie, R. and De Weer, P. (1978) Am. J. Physiol. 235, C63–C68.
13 Eisner, D.A. and Lederer, W.J. (1980) J. Physiol. (London) 303, 441–474.
14 Gadsby, D.C. (1984) Annu. Rev. Biophys. Bioenerg. 13, 373–398.
15 Lederer, W.J. and Nelson, M.T. (1984) J. Physiol. (London) 348, 665–677.
16 De Weer, P., Gadsby, D.C. and Rakowski, R.F. (1986) J. Physiol. (London) 371, 144P.
17 Lafaire, A.V. and Schwarz, W. (1986) J. Membrane Biol. 91, 43–51.
18 Forbush III, B. (1984) Proc. Natl. Acad. Sci. USA 81, 5310–5314.
19 Fendler, K., Grell, E., Haubs, M. and Bamberg, E. (1985) EMBO J. 4, 3079–3085.
20 Karlish, S.J.D., Kaplan, J.H. (1985) in The Sodium Pump (Glynn, I. and Ellroy, C., eds.), pp. 501–506, Company of Biologists, Cambridge, U.K.
21 Borlinghuas, R.T., Apell, H.-J., Läuger, P. (1987) J. Membrane Biol. 97, 161–178.
22 Apell, H.-J., Borlinghaus, R.T., Läuger, P. (1987) J. Membrane Biol. 97, 179–191.
23 Jørgensen, P.L. (1974) Methods Enzymol. 32, 277–290.
24 Schwartz, A., Nagano, K., Nakao, M., Lindenmayer, G.E. and Allen, J.C. (1971) Methods Pharmacol. 1, 361–388.
25 Läuger, P., Lesslauer, W., Marti, E. and Richter, J. (1967) Biochim. Biophys. Acta 135, 20–32.
26 Kaplan, J.H., Forbush III, B. and Hoffman, J.F. (1978) Biochem. 17, 1929–1935.
27 McCray, J.A., Herbette, L., Kihara, T. and Trentham, D.R. (1980) Proc. Natl. Acad. Sci. USA 77, 7237–7241.
28 De Luca, M. and McElroy, W.D. (1978) Methods Enzymol. 57, 3–15.
29 Garay, R.P. and Garrahan, P.J. (1973) J. Physiol. (London) 231, 297–325.
30 Blostein, R. (1983) J. Biol. Chem. 258, 7948–7953.
31 Forgac, M. and Chin, G. (1982) J. Biol. Chem. 257, 5652–5655.
32 Karlish, S.J.D., Rephaeli, A. and Stein, W.D. (1985) in The Sodium Pump (Glynn, I. and Ellroy, C., eds.), pp. 487–499, Company of Biologists, Cambridge, U.K.
33 Apell, H.-J. and Marcus, M.M. (1986) Biochim. Biophys. Acta 862, 254–264.
34 Nagel, G., Fendler, K., Grell, E. and Bamberg, E. (1987) Biochim. Biophys. Acta 901, 239–249.
35 Karlish, S.J.D., Gates, D.W. and Glynn, I.M. (1978) Biochim. Biophys. Acta 525, 252–264.
36 Hegyvary, C. and Post, R.L. (1971) J. Biol. Chem. 264, 5234–5240.